Comparisons of predictions from two intranuclear-cascade models with measured secondary proton spectra at several angles from 62- and 39-MeV protons on various elements*

H. W. Bertini
Neutron Physics Division, Oak Ridge National Laboratory, Oak Ridge, Tennessee 37830

G. D. Harp
Chemistry Department, Brookhaven National Laboratory, Upton, New York 11973

F. E. Bertrand
Physics Division, Oak Ridge National Laboratory, Oak Ridge, Tennessee 37830
(Received 5 August 1974)

Detailed comparisons of correlated energy-angle proton spectra corresponding to continuum state transtions have been made between experimental data and two versions—Brookhaven National Laboratory (BNL) and Oak Ridge National Laboratory (ORNL)—of the intranuclear-cascade model for 62- and 39-MeV protons incident on carbon, iron, and bismuth. These energies were selected because detailed experimental data are available and because the energy limit of validity of the intranuclear-cascade approach could be examined. The calculated spectra are in good agreement ($\lesssim 30\%$) with the shapes and magnitudes of the measured integral spectra for the 62-MeV reactions. However, the comparisons of the spectra at angles $\lesssim 20°$ and $> 90°$ are poor. There is a much greater discrepancy in the correlated energy-angle data from reactions at 39 MeV. The BNL version, which contains the greater physical detail, tends to reduce the discrepancies in the spectral shape at small and large angles between the experimental data and the simpler intranuclear-cascade version (ORNL). Examples of these discrepancies are: a high estimated quasifree peak at small angles and a small scattering intensity at back angles. However, the BNL version reduces the particle yield for heavy targets so that the comparisons of the predicted absolute cross sections with the experimental data are often poor. The effects of reflection and refraction, which are included in the BNL version only, appear to be in the right direction to compensate for the discrepancies of the ORNL version, but some modification in the manner that this phenomenon is incorporated may be required to avoid the discrepancies in absolute cross sections.

[NUCLEAR REACTIONS $^{12}C(p, p'X)$, $^{54}Fe(p, p'X)$, $^{209}Bi(p, p'X)$ calculated $\sigma(E; E_{p'}, \theta)$, $\sigma(E)$; $E = 39$, 62 MeV. Intranuclear-cascade models.]

I. INTRODUCTION

The intranuclear-cascade model (INC) is a relatively simple semiclassical nuclear model that is widely used for the description of continuum state transitions in high-energy (>100 MeV) nucleon-induced nuclear reactions.[1-3] One version of this model has recently been shown to yield unexpectedly good results for the nonelastic cross section σ_R when compared to data from lower energy (30–60 MeV) proton-induced reactions.[4] This fact and the recent interest in continuum-region calculations[5] encouraged a comparison between some recent low-energy experimental data[6] and two commonly used versions of the INC model. In addition, the completeness of the experimental data for 30- and 60-MeV protons permits a more detailed comparison of the effects of the different physical properties incorporated in the two versions than has been possible before.

One of the two versions of the INC model discussed in this paper was developed at the Oak Ridge National Laboratory (ORNL version),[3,7] and the other was developed in a joint effort at Columbia University and at the Brookhaven National Laboratory (BNL version).[2,8] In general, the BNL version includes a more detailed representation of a real reaction process than does the ORNL version.

II. MODEL

A. General description

The intranuclear-cascade model is based on the assumption that the reactions of incident particles with complex nuclei can be represented by a sequence of two-particle interactions that take place within a model nucleus. A brief description of the calculational method is given here with details given elsewhere.[2,7,8] The nucleus is considered to be a modified zero-temperature Fermi energy state. An incident particle is made to enter the nucleus and, if it collides with one of the target nucleons,

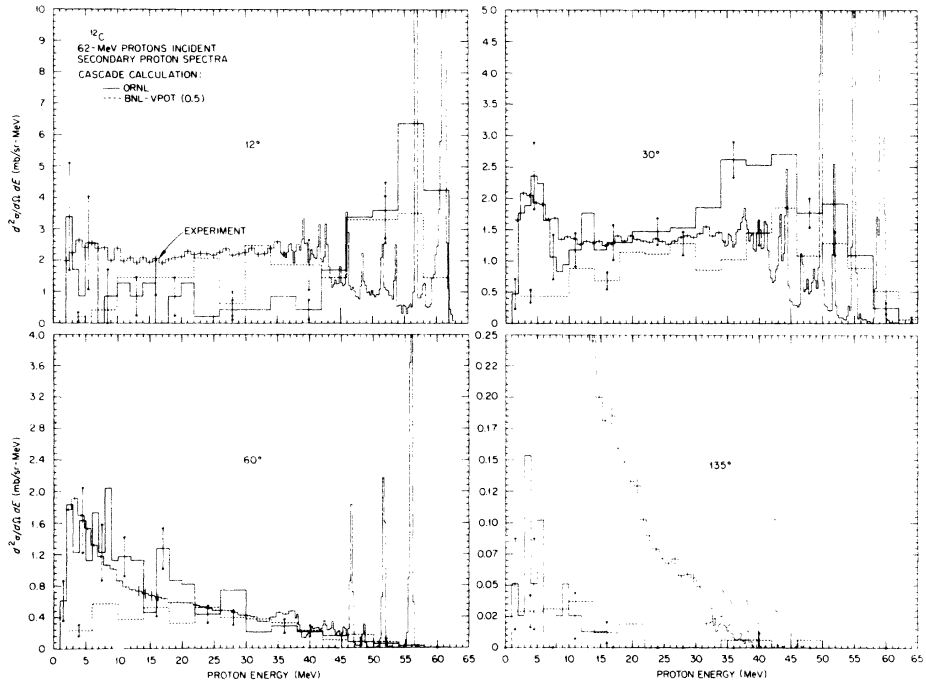

FIG. 1. Secondary proton spectra from 62-MeV protons on ^{12}C. The angular intervals used for the ORNL and BNL calculations were 11–13° for the data illustrated at 12°, 27–33° for the 30° data, 58–62° for the 60° data, and 126–146° for the 135° data.

it is assumed that the collision can be described as a free-particle collision. Free-particle differential-scattering cross sections, in conjunction with Monte Carlo techniques, are used to determine the interaction probability and the scattering angle. Relativistic kinematics are used to determine the vector momenta of the scattered and recoil nucleons in the laboratory system. The energies of the scattered nucleons are examined to approximately account for the exclusion principle and, if there is no violation of this principle, the calculation proceeds. The path of each of these nucleons is followed, one at a time, to the next collision site where the process is repeated, thus developing a cascade. The energy-dependent free-particle scattering and differential cross sections exclusive of p-p Coulomb scattering are used to determine the collision site and the scattering angle. The "history" of each nucleon involved in the cascade is traced until the nucleon either escapes or until its energy becomes so low that it is assumed to be trapped within the nucleus. A record is kept of the information pertinent to each escaping particle, such as the type of particle (neutron or proton), its vector momentum, etc. Thousands of such incident-particle and induced-cascade histories are followed in order to generate statistically significant results. Transitions to the eigenstates of any intermediate nuclei are not taken into account since the Fermi gas states of these nuclei are not quantized. Recombinations of holes and particles and the decay of the holes are not included in these models.

From the records kept of the vector momenta of the escaping particles, energy spectra may be constructed for any angular interval, and post-cascade excitation energy distributions can be obtained for various possible residual nuclei. The correlated angle-energy distributions of the escaping particles are given in absolute units, and direct comparisons with experimental data on an absolute basis can be made. Once the parameters of the calculation are set, they can remain fixed (as they were for this report) for all results from all targets at all energies.

The excitation energies of the residual nuclei are assumed to be given up by equilibrium processes. These processes will not be discussed here because the different assumptions used in their calculation make comparisons between the ORNL and BNL versions difficult to interpret. The excitation energy distributions from the two versions have been compared elsewhere.[9]

B. Nuclear properties of the models

The ORNL and BNL versions ascribe somewhat different properties to the nucleus. Calculations indicate that the effect of these differences does not have a noticeable effect on the results,[9] so only

a brief description will be given here.

The nucleus is assumed to be spherically symmetric, consisting of a dense central core surrounded by annular regions of diminishing density. The density within each region is assumed to be constant. There are three annular regions in the ORNL version and seven in the BNL version. The energy distribution of the bound nucleons in the nucleus was taken to be a zero-temperature Fermi distribution. The maximum kinetic energies of the protons and neutrons in each region are thereby determined from their densities in each region.

The single-particle potential for the protons, and similarly for the neutrons, in each region in the ORNL version was taken to be $-(E_f+7)$ MeV, where E_f is the proton Fermi energy in the region and the 7 MeV is an approximation to the separation energy of the neutrons and protons for all nuclei. In the BNL version, the separation energy was taken to be the average of the separation energies for the removal of a proton and for the removal of a neutron from the target nucleus. In addition, the dependence of the potential depth on the energies of the incident and emergent particles was included.

An approximation to the exclusion principle is invoked by comparing the energies of the neutrons and protons after every collision with the neutron or proton Fermi energy of the region in which the collision has taken place. If the energy of either particle is below the Fermi energy, the reaction is "forbidden," the collision is ignored, and the nucleon that initiated the collision is allowed to proceed to its next estimated collision site. The cutoff energy is the nucleon kinetic energy inside the nucleus beyond which the cascade process is no longer followed. It is of the order of the depth of the single-particle potential plus the Coulomb potential. When the energy of the particle falls below the cutoff energy, the particle is assumed to be trapped, wherein it becomes part of the residual nucleus.

C. Dynamical properties

The following dynamical properties refer only to the BNL version; none of them is included in the ORNL version: (1) The classical trajectories of all of the particles are altered at the region bound-

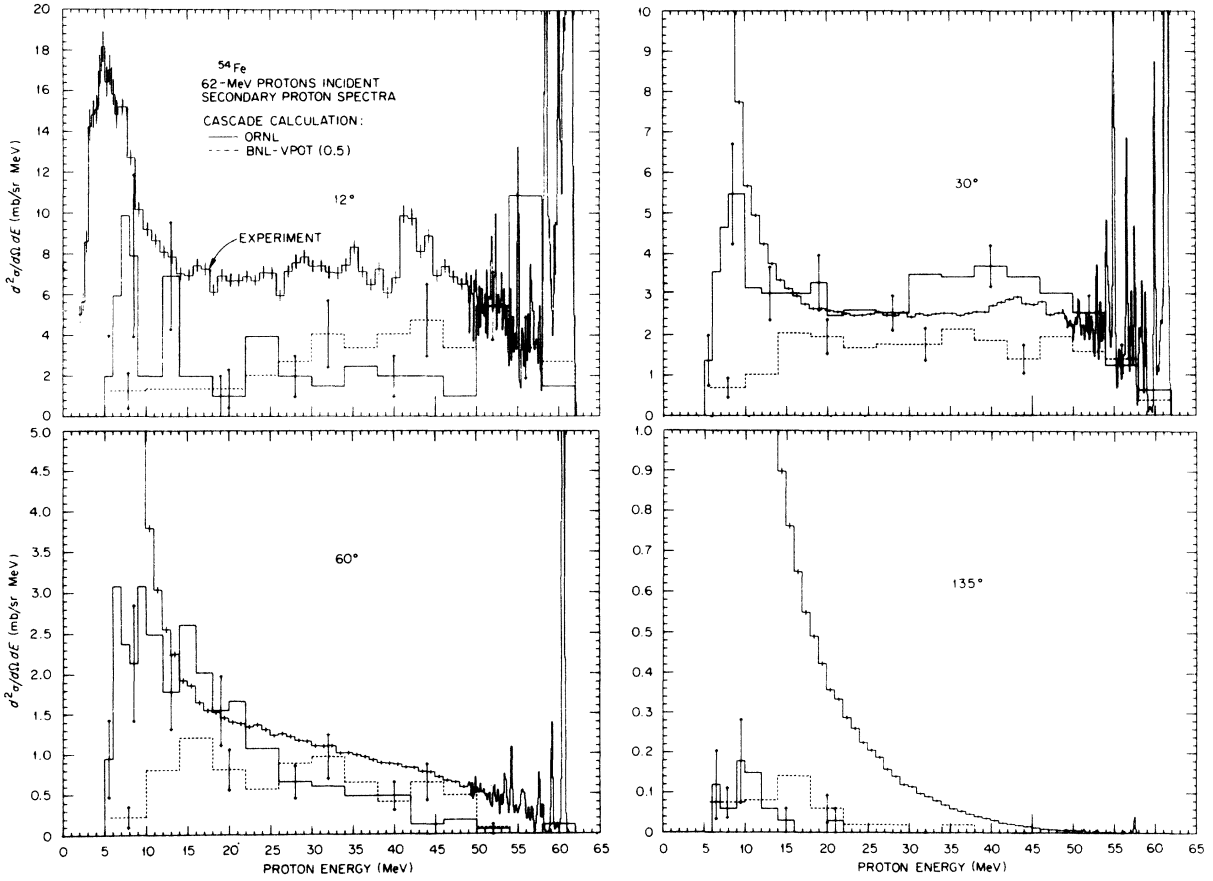

FIG. 2. Secondary proton spectra from 62-MeV protons on ^{54}Fe. The angular intervals used for the calculations are the same as those described in Fig. 1.

aries to account for refraction and reflection by an energy-dependent nuclear potential. (2) The effects of nucleon-pair correlations are approximately accounted for by preventing two sequential scatterings from taking place within a distance d of each other. The results are somewhat insensitive to the value of d (described in Ref. 2), and a value of 0.5 fm was used for this paper.

To calculate the refraction, it is assumed that only the radial component of the particle momentum, p_r, is changed, while its tangential component remains unaltered. Assuming that $E^2 - p^2$ is invariant, then

$$p_r'^2 = p_r^2 + E'^2 - E^2 ,$$

where E is the total energy and the primed and unprimed values refer to the new and old regions of potential, respectively. E' is given by

$$E' = E - (V' - V) ,$$

where V' and V are the potentials in the new and old regions. In order to conserve the tangential component of the momentum, the angle of refraction is given by

$$\frac{\sin\theta}{\sin\theta'} = \frac{p'}{p} .$$

The critical angle for total reflection θ_{cr} is given by the condition that $\sin\theta' = 1$, or

$$\cos\theta_{cr} = \frac{(E^2 - E'^2)^{1/2}}{p} .$$

The complexities that occur for the treatment of mesons have been omitted for this discussion.

III. COMPARISON WITH EXPERIMENTAL DATA

A. 62-MeV incident protons

The experimental data of Bertrand and Peelle[6] were selected for comparative purposes because these data spanned the entire secondary energy region and covered a large range of target masses and angles of observation. The BNL calculation used in these comparisons was the version designated as VPOT (0.5) which indicates that velocity-dependent potential and pair correlation effects

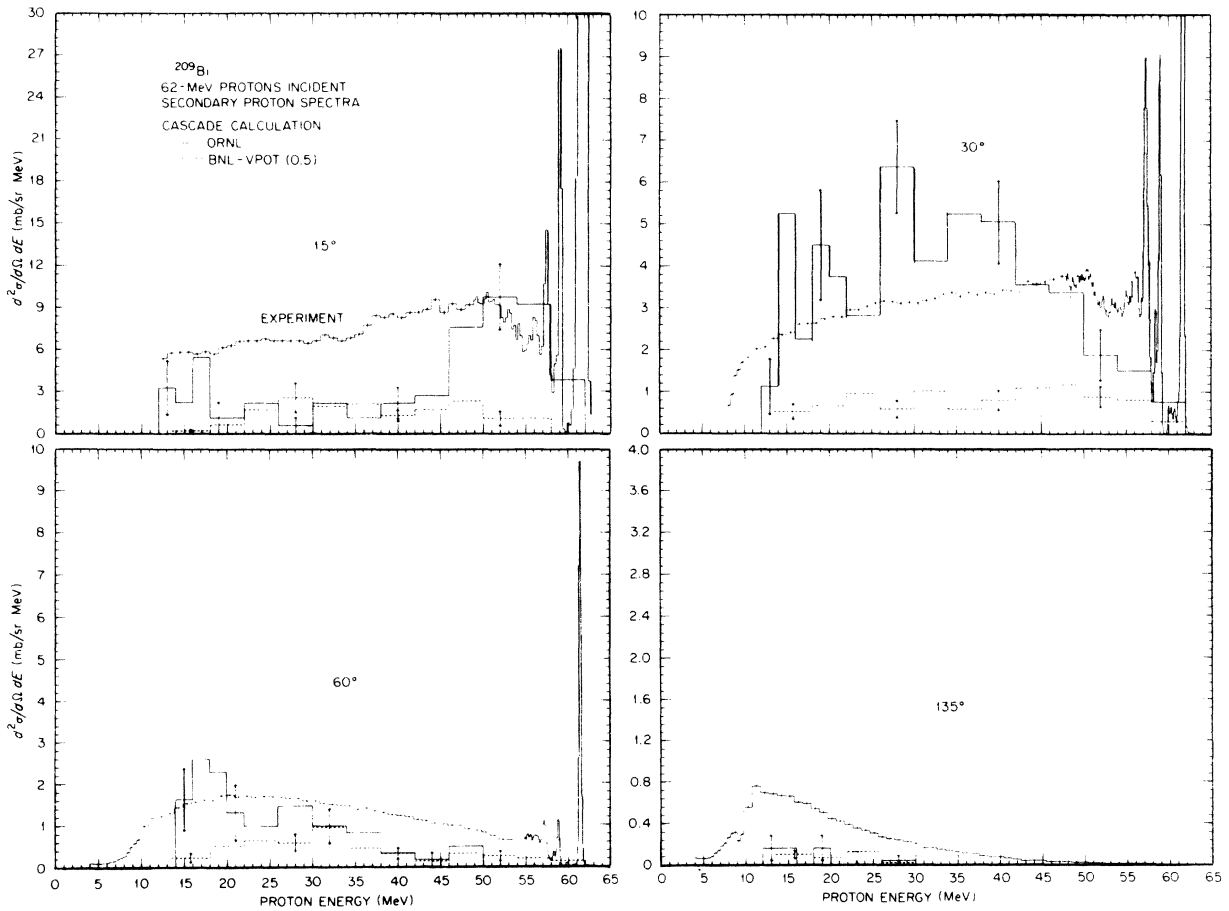

FIG. 3. Secondary proton spectra from 62-MeV protons on ^{209}Bi. The angular interval used in the calculations for the data illustrated at 15° was 13–17°. At other angles, the same intervals described in Fig. 1 were used.

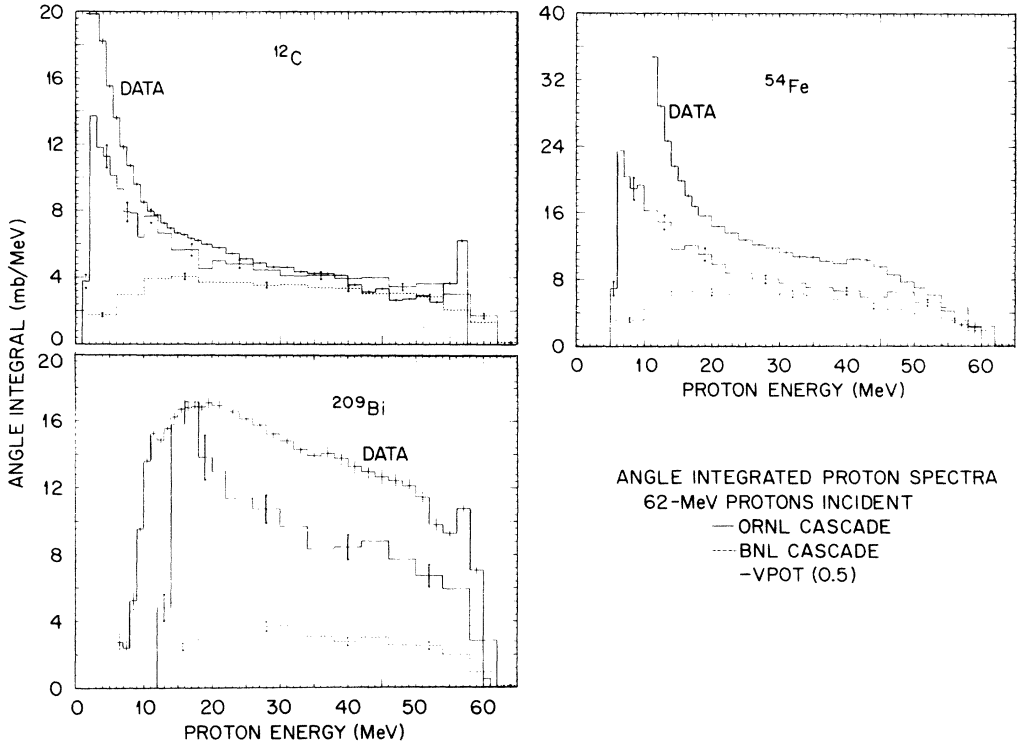

FIG. 4. The secondary proton spectra integrated over all angles for 62-MeV protons on carbon, iron, and bismuth. Elastic scattering has been omitted.

were included.

Figures 1–3 show the spectra of secondary protons at various angles from 62-MeV protons on carbon, iron, and bismuth. The sharp peaks in the experimental data at the high energies are produced by single-step inelastic nuclear scattering reactions leading to low-lying levels of the residual nucleus; the details of these reactions are not included in the INC calculations. The highest energy peaks observed in Figs. 1–3 are from elastic scattering, which is not considered in the calculations. Many of the elastic, the inelastic, and the evaporation peaks are off scale in the figures, but these reactions are not pertinent to this report. Typically, at the small angles the ORNL version yields a large high-energy quasifree scattering peak near the free-particle nucleon-nucleon scattering energy, and there is a dip in the predicted spectra below the experimental data at midrange energies, whereas the BNL version shows a suppressed or smeared quasifree peak at these angles and hence a better reproduction of the shapes of the spectra. The elimination of the quasifree peak in the BNL calculation is a direct result of the inclusion of reflection and refraction.[8] This process tends to "wash out" the kinematics of the proton-nucleon collision process compared to the ORNL version. Thus, while the single-step quasifree scattering process provides a considerable fraction of the higher energy cross sections, the results from the BNL version for this process are not manifested in a peak, as shown in Figs. 1–3. At 30 and 60° the ORNL version is generally in better agreement with the experimental data. At the back angles both versions grossly underestimate the experimental data, but the BNL version yields some high-energy protons scattered backwards while the ORNL version does not. Again, the reflection and refraction process included in the BNL version is responsible for the enhanced production of protons at back angles. In defense of the INC calculations, it should be pointed out that the cross section over the angular range from about 20 to 75 encompasses about 75% of the total nonelastic cross section, and in this angular range the predicted spectra are in reasonable agreement with the experimental data.

The nonelastic energy spectra integrated over all angles from 62-MeV incident protons are shown in Fig. 4. The ORNL version reproduces both the shape and the magnitude of the experimental data better than does the BNL version, even though the BNL version provides a better reproduction of the shapes of the differential spectra by the elimination of the quasifree peak. The small yield at low energies in the spectra from the BNL version is

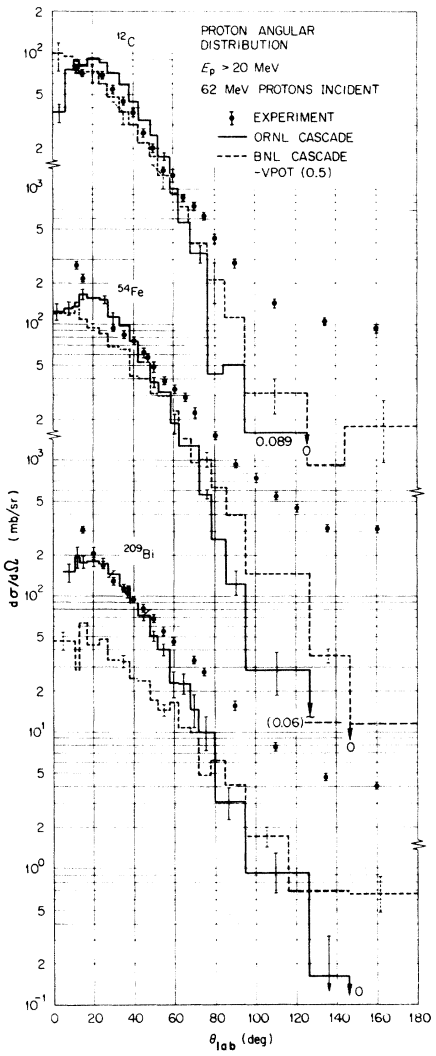

FIG. 5. The angular distribution of nonelastic protons with energies > 20 MeV for 62-MeV protons on carbon, iron, and bismuth.

caused by the reflection of low-energy cascade protons back into the nucleus when these protons strike the interior of the potential surface at angles greater than the critical angle. Reflections at the interior nuclear surface also account for the drop in the intensity of the yield for the heavy targets.

Figure 5 contains the angular distributions for protons emitted from carbon, iron, and bismuth with energies >20 MeV. The 20-MeV cutoff ensures that the experimental cross sections shown are nonevaporation. Except at the wide angles, the ORNL version reproduces the magnitude of the cross sections better than does the BNL version. The former version shows a dip at the smallest angles, whereas the latter does not. The dip is caused by exclusion effects; i.e., at small angles where energy transfers are also small, it becomes less probable for both an incident and a target nucleon to be above the Fermi sea after a collision. Although the same effect applies in the BNL version, it is compensated for by the refraction of particles into the small-angle region from particles that would normally have been emitted at wider angles.

B. 39-MeV incident protons

It has often been expected that the underlying concepts of the intranuclear-cascade approach, such as the spatial localization of the incident and scattered particles and the assumption of two-body collisions, would become less applicable as the incident energy is lowered. Comparisons are made at 39 MeV to illustrate the extent that these concepts still apply.

Figures 6–8 illustrate the proton energy spectra at various angles from 39-MeV protons on carbon, iron, and bismuth. Discrepancies similar to those observed with the 62-MeV incident protons appear but with an intensification of the discrepancy caused by the quasifree peak in the ORNL version. As is seen in Figs. 6–8, the contribution to the total cross section from direct inelastic excitation of low-lying levels in the nucleus increases as the energy of the incident projectile decreases. Since no attempt is made to calculate the cross sections for scattering to the discrete states in the INC programs, the differential spectral comparisons with the INC calculation show considerable disagreement, particularly for light nuclei. However, while the calculation does not localize the cross section in discrete states, it does account for the total nonelastic cross section (i.e., integrated over energy). Hence, the low-energy limitation of the model may be determined when the inelastic spectra are dominated by the single-step excitation of low-lying states.

Figure 9 shows the nonelastic energy spectra integrated over all angles where, in the case of a bismuth target, the BNL version grossly underestimates the data. At high energies the measured integrated spectra show the effects of direct excitation of low-lying levels. These effects are less obvious in the angle-integrated spectra than in the energy spectra at specific angles due to the kinematic smearing in the laboratory system integration over angle.

Figure 10 illustrates the angular distribution for nonevaporation protons emitted with energies >15 MeV where the discrepancies of the BNL version for the heavier targets are larger than at 60 MeV, as would be expected if the difficulty is produced by total internal reflection.

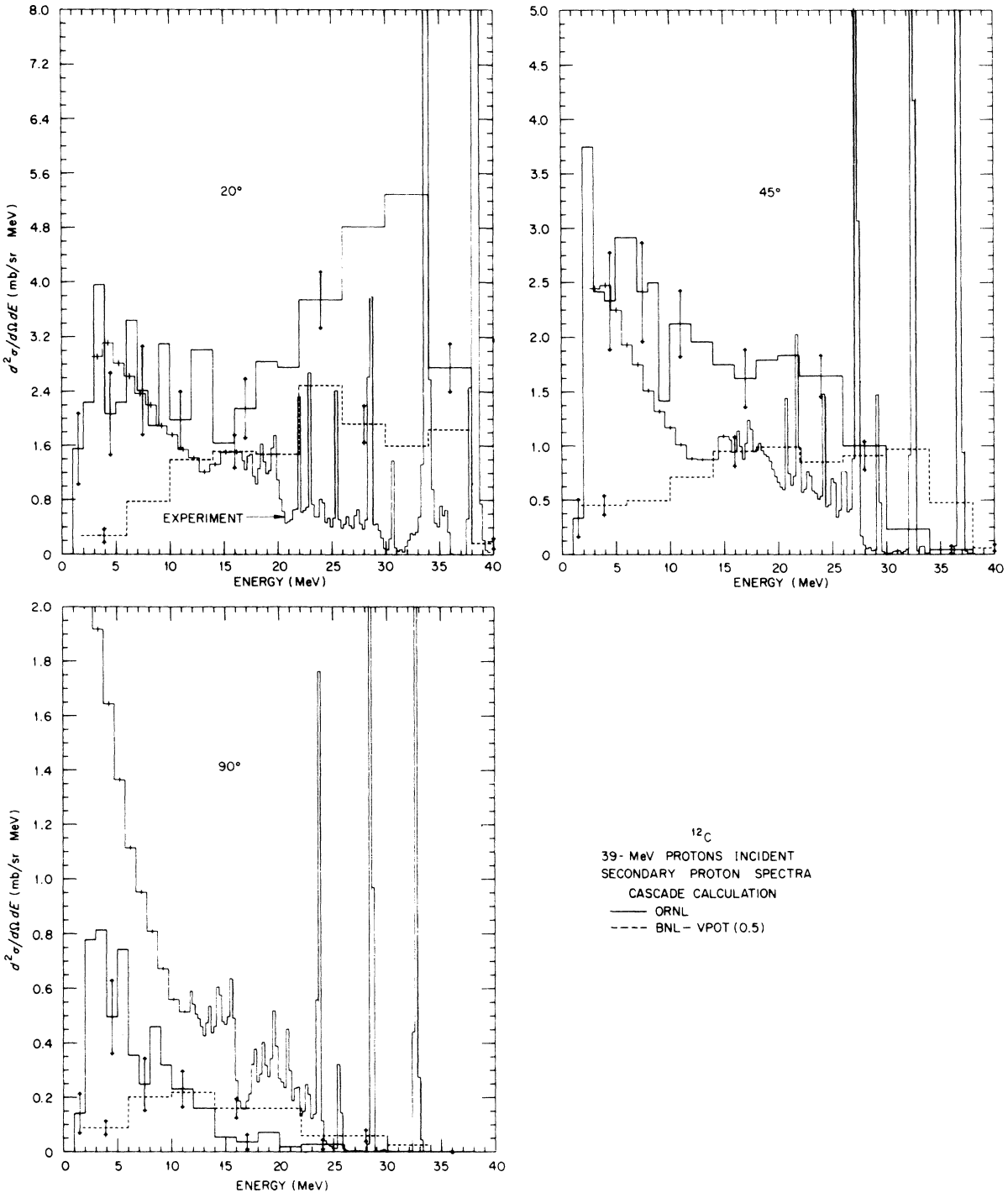

FIG. 6. Secondary proton spectra from 39-MeV protons on ^{12}C. The angular intervals used in the ORNL and BNL calculations were 17–23° for the data illustrated at 20°, 42–48° for the data at 45°, and 85–95° for the data at 90°.

C. Coulomb effects

The effect of the Coulomb potential on the particle spectra was also investigated. The angle of deflection of the incident protons by the nuclear Coulomb potential was calculated classically assuming a target nucleus of infinite mass. The emergent secondary protons were similarly de-

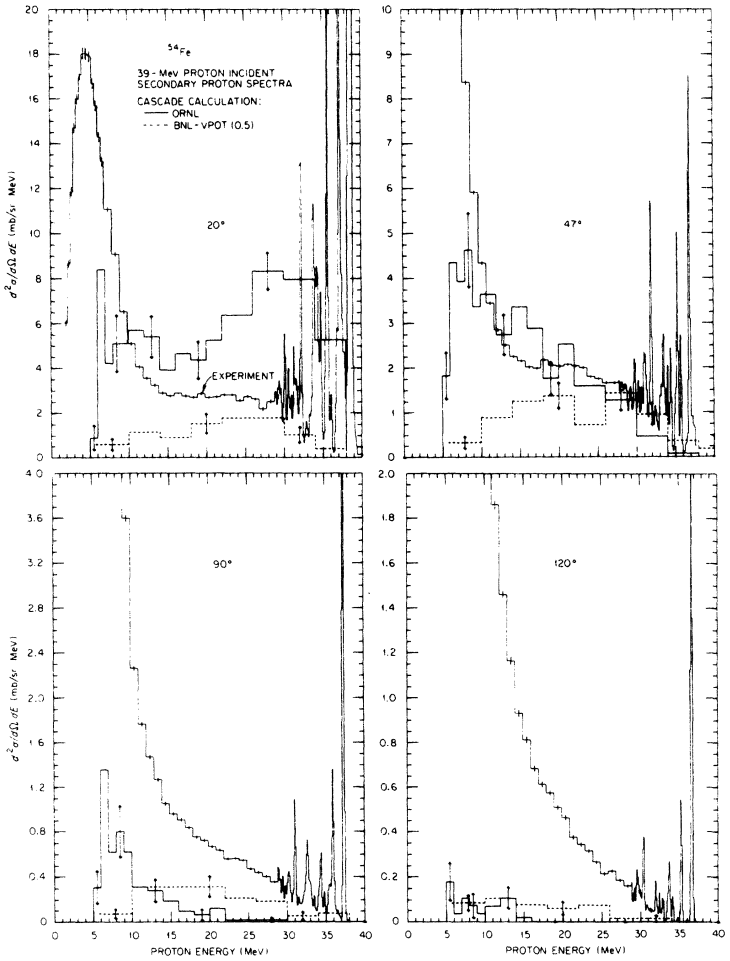

FIG. 7. Secondary proton spectra from 39-MeV protons on ^{54}Fe. The angular interval used in the calculations for the data at 47° was 44–50°, and for the data at 120° it was 110–130°. The same angular intervals described in Fig. 6 were used for the data illustrated at 20° and 90°.

flected; i.e., scattered and recoil cascade nucleons can originate anywhere within the nucleus, and they can be traveling in a variety of directions as they escape from the nucleus. When charged particles (protons) escape they experience the Coulomb force, which is directed radially from the center of the nucleus. The direction of the escaping protons is thus altered, and the angular distribution is also altered. For all of the cases considered in this paper, the only reaction where Coulomb effects changed the results beyond the usual statistical variation was that for 39-MeV protons on bismuth, and these results are shown in Fig. 8 as solid circles. These data should be compared with the results from the ORNL version. The Coulomb calculations were carried out in conjunction with a BNL-STEPNO program, which is essentially equivalent to the ORNL version.

Although the agreement with experimental data is enhanced, the effective "geometric" cross section was reduced by 35% because the incident protons with large impact parameters completely miss the target as a result of Coulomb deflection. It has been demonstrated that the INC calculation[4] (ORNL version or BNL-STEPNO) without Coulomb effects can predict the total nonelastic cross section for this reaction quite well. Thus, in this case, the inclusion of physical properties known to be important to nuclear reactions tends to improve the spectral agreement but reduces the agreement for the reaction cross section.

IV. DISCUSSION

While the INC calculation compares poorly to the small-angle and large-angle data, the calculation does provide a rather good description of the bulk of the results. As is seen in Figs. 4 and 9, the calculation reproduces the shapes of the measured spectra well and it reproduces the magnitude to

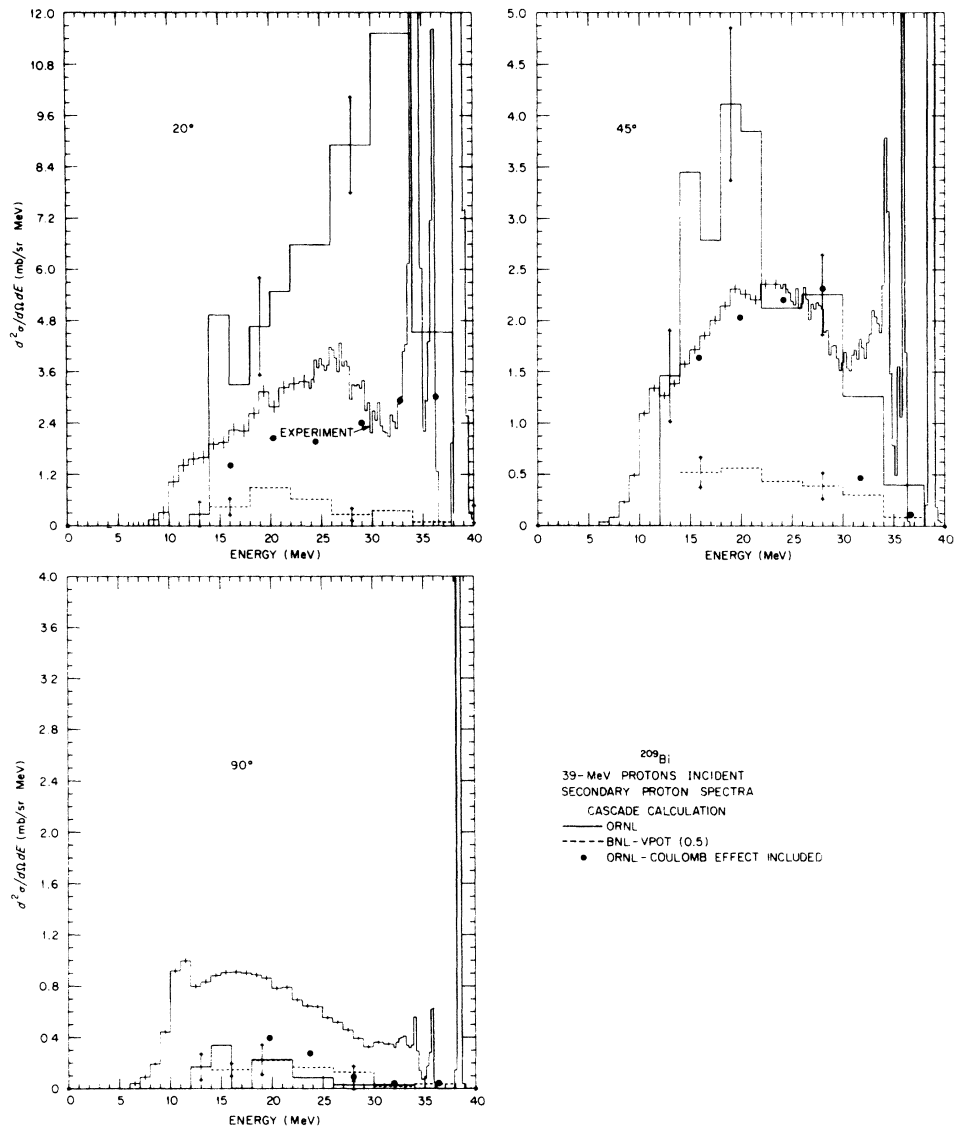

FIG. 8. Secondary proton spectra from 39-MeV protons on ^{209}Bi. The angular intervals used for the calculations were the same as described in Fig. 6.

25–30%. The fact that the comparisons are as good as they are may indicate that the long-assumed energy limit of the calculation based on the de Broglie wavelength of the incident particle may not be appropriate. Rather, the limitation may be reached when the spectra are dominated by direct excitations of low-lying processes and purely equilibrium processes.

Of the additional physical properties introduced in the BNL calculations, refraction and reflection appear to have the greatest effect on the correlated energy-angle spectra. At the energies under consideration this property suppresses the quasifree peak at small angles in agreement with measurements, and it allows the emission of more nearly the correct fraction of fast particles at back angles. However, as presently formulated, the inclusion of reflection and refraction suppresses the escape of particles to the extent that serious discrepancies in magnitude are introduced for all of the elements at the lower incident energies and for the heavier elements at all energies considered. Thus, when the knowledge of the most realistic absolute cross sections below ~100 MeV is important, utilization of the BNL version without reflection and refraction would be appropriate. An additional investigation of this property would be in order.

The ORNL version was temporarily modified to examine the effect of scattering from clusters of nucleons within the nucleus to see if scatterings

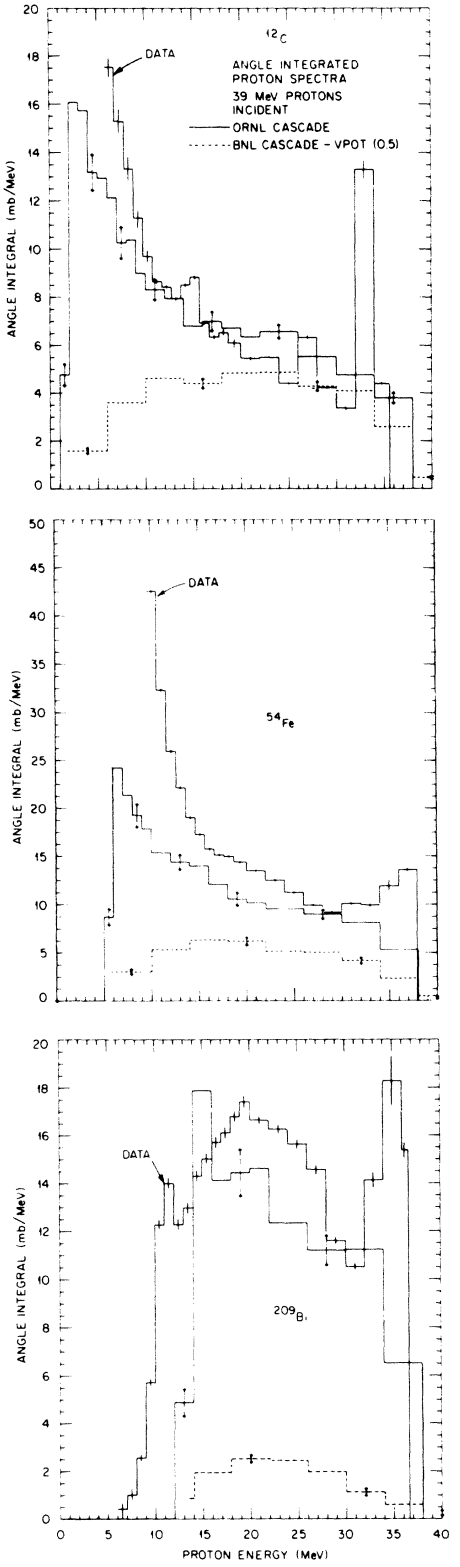

FIG. 9. The secondary proton spectra integrated over all angles for 39-MeV protons on carbon, iron, and bismuth. Elastic scattering has been omitted.

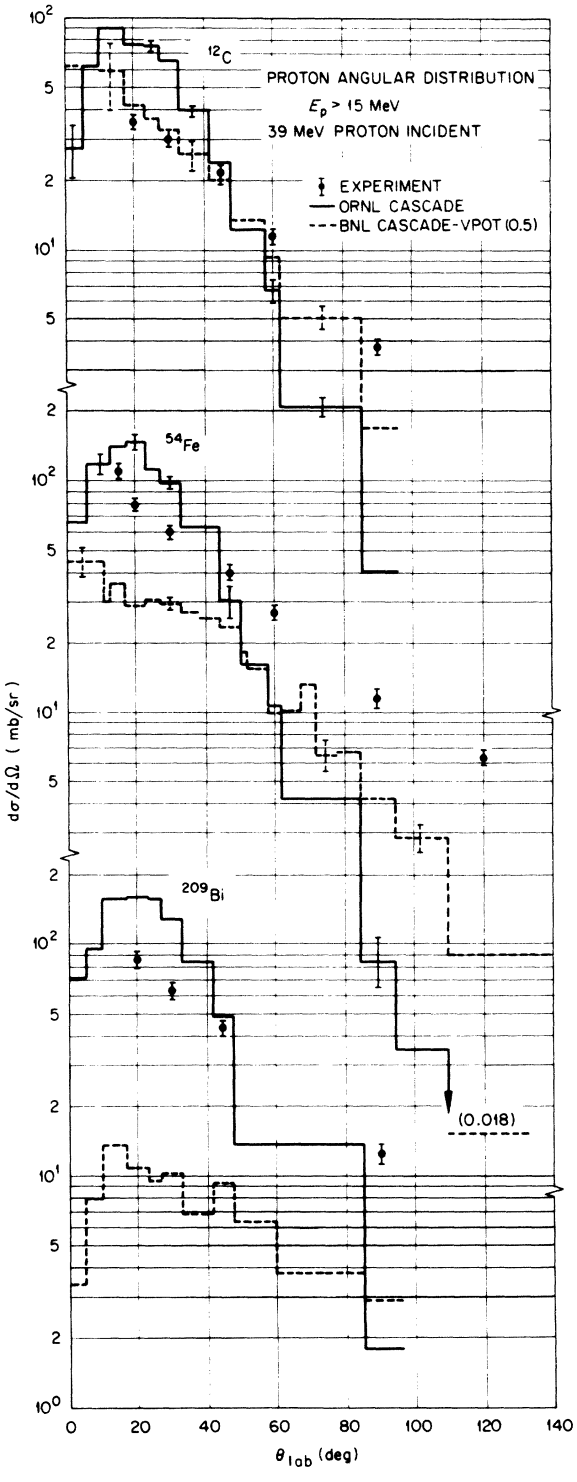

FIG. 10. The angular distribution of nonelastic protons emitted with energies > 15 MeV from 39-MeV protons on carbon, iron, and bismuth.

from these heavier "particles" would alleviate the discrepancy in the spectra at back angles by enhancing the scattering intensity in the backward direction.[6] The scatterings within the nucleus were forced to be made with particles of mass 4 and mass 2. The enhancement was such that the back angle experimental spectra were reproduced quite accurately. This finding opens another area of investigation that might prove fruitful. In this vein, it is possible that the inclusion of reactions with correlated clusters of nucleons (both scattering and breakup reactions) could considerably strengthen the foundations of the model, as well as increase its general utility.

There is the potential, within the INC approach, to calculate the interaction of cascade nucleons with holes, to permit hole decay, and to calculate transitions to the eigenstates of the residual nucleus. This has not been done anywhere, to our knowledge.

Other models, notably the preequilibrium models,[10] have been investigated for their applicability in this transition energy range where the nuclear reactions are clearly not compound, nor are they completely single-step reactions either. These models approach the problem from a statistical point of view, and they presently yield only angle-integrated spectra. It is somewhat difficult to evaluate the models based on comparisons with angle-integrated spectra alone, because this is tantamount to investigating the various intranuclear-cascade approaches by the examination of only Figs. 4 and 9. If this were done, one would lose considerable insight into both the specific causes of the discrepancies and the modifications that might be required to validate the models.

---

*This work was partially funded by the National Aeronautics and Space Administration, Order H-38280A, under Union Carbide Corporation's contract with the U.S. Atomic Energy Commission and by the Brookhaven National Laboratory, Associated Universities, Incorporated, under contract with the U.S. Atomic Energy Commission.

[1]V. S. Barashenkov, K. K. Gudima, and V. D. Toneev, Acta Phys. Pol. 36, 887 (1969).

[2]K. Chen, G. Friedlander, G. D. Harp, and J. M. Miller, Phys. Rev. C 4, 2234 (1971).

[3]H. W. Bertini, Phys. Rev. C 6, 631 (1972).

[4]H. W. Bertini, Phys. Rev. C 5, 2118 (1972).

[5]G. R. Satchler, Nucl. Phys. A195, 1 (1972); M. B. Lewis and F. E. Bertrand, *ibid.* A196, 337 (1972).

[6]F. E. Bertrand and R. W. Peelle, Phys. Rev. C 8, 1045 (1973).

[7]H. W. Bertini, Phys. Rev. 131, 1801 (1963).

[8]K. Chen, G. Friedlander, G. D. Harp, and J. M. Miller, Phys. Rev. 166, 949 (1968); K. Chen, G. Friedlander, and J. M. Miller, *ibid.* 176, 1208 (1968).

[9]V. S. Barashenkov, H. W. Bertini, K. Chen, G. Friedlander, G. D. Harp, A. S. Ilienov, J. M. Miller, and V. D. Toneev, Nucl. Phys. A187, 531 (1972).

[10]J. J. Griffin, Phys. Rev. Lett. 17, 478 (1966); G. D. Harp, J. M. Miller, and B. J. Berne, Phys. Rev. 165, 1166 (1968); M. Blann, Phys. Rev. Lett. 21, 1357 (1968); C. K. Cline, Nucl. Phys. A174, 73 (1971); M. Blann, Phys. Rev. Lett. 28, 757 (1972); G. M. Braga-Marcazzan, Phys. Rev. C 6, 1398 (1972); H. Feshbach, Rev. Mod. Phys. 46, 1 (1974).